



ISSN: 0067-2904

Utilization of Magnetic Mesoporous Silica (Fe₃O₄@mSiO₂) in Adsorption, Loading, and Release Kinetics of Diphenhydramine Drug

Enaas Abdul Hussein, Sameer H. Kareem, Inaam H. Ali*

Department of Chemistry, College of Science for women, University of Baghdad, Baghdad, Iraq

Abstract

The current study uses mesoporous silica magnetic Fe₃O₄@mSiO₂ nanoparticles as core-shell materials to deliver the drug diphenhydramine (DPH). To investigate the DPH drug's adsorption behavior in aqueous solutions, the batch approach has been employed. The adsorption evaluations that were obtained were fitted with the Langmuir, Freundlich, Temkin, and Dubinin-Radushkevich isotherms models. According to the results, the Freundlich model was the best fit for the data, and the type of adsorption process used was physical. After kinetic analysis, it was discovered that the data agreed quite well with the pseudo-second-order kinetic equation. The Fe₃O₄@mSiO₂ carrier's DPH drug loading capacity and release kinetics were also examined. The calculated amount of DPH loaded on the sample was 13.33 mg drug/mg sample. The release profiles of the loaded Fe₃O₄@mSiO₂ sample show that the DPH release percentage in the water and (phosphate buffer solution) PBS solution is 57.23 and 97.27%, respectively. The release kinetics was also studied using three models: Korsmeyer-Peppas, first-order kinetic release, and Kopcha. The results indicate that the Kopcha model conforms more closely to the data release than other models.

Keywords: Adsorption isotherm, Fe₃O₄@mSiO₂, Mesoporous silica, DPH, Drug delivery.

استخدام سیلیکا متوسطة المسام مغناطیسیة $(Fe_3O_4@mSiO_2)$ في امتزاز وتحمیل وحرکیة تحرر دواء دای فنیل هایدرامین

ايناس عبد الحسين خضير، سمير حكيم كريم ، انعام حسين علي * قسم الكيمياء، كلية العلوم للبنات، جامعة بغداد، بغداد، العراق

الخلاصة

استخدم في الدراسة الحالية دقائق نانوية مغناطيسية من سيليكا متوسطة المسام كمواد حاملة لدواء داي فنيل هايدرامين. تم دراسة السلوك الامتزازي لدواء DPH في الانظمة المائية بطريقة الدفعات. تم تطبيق معادلات امتزاز مثل لنكماير، فرندلج، تمكن و دوبنين ورادسكوفج ووفقا للنتائج كانت معادلة فرندلج الافضل تطابقا للبيانات مع وان عملية الامتزاز من النوع الفيزياوي. تم تحليل بيانات حركية الامتزاز وكانت متطابقة مع معادلة الدرجة الثانية الكاذبة. تم دراسة قابلية تحميل وحركية تحرر دواء DPH على سطح Fe₃O₄@mSiO₂ فكانت

*Email: inaam.mohmmed@gmail.com

كمية الدواء المحملة 13.33 ملغم لكل ملغم من النموذج المحضر. بينما كانت نسبة DPH المتحرر من سطح النموذج في الماء وفي محلول البغر هي 57.23% و 97.27% علي التوالي, حركية تحرر الدواء تم دراستها بأستخدام ثلاث معادلات هي: كورسماير – بيباس و حركية تحرر الدرجة الاولى و معادلة كوبجا. اثبتت النتائج ان معادلة كوبجا اعطت تطابقا مع بياتات تحرر الدواء اكثر من باقي المعادلات.

1. Introduction

The idea of drug delivery is the transfer, within a set amount of time, of a particular dosage of various medicinal products, such as genes, proteins, and drugs, to the target site in the body [1,2]. Moreover, drug carriers deliver lipophilic and hydrophilic medications to fulfill the system's intended use, improve the pharmacokinetic effect, and shield the medicinal agent from enzyme degradation [3,4]. Mesoporous silica is a novel drug carrier with exceptional characteristics, including biocompatibility, a high loading capacity owing to its large pore volume and specific surface area, and adjustable pore size [5-8]. Recently, there has been a growing interest in mesoporous silica core-shell nanocomposites. [9]. Combining them with a magnetic core not only provides assistance in controlling these carriers, but also allows mesoporous silica to construct effective vehicles. According to Yang et al. [10], mesoporous Fe₃O₄@mSiO₂ core-shell nanocomposites (approximately 65 nm) loaded with doxorubicin (DOX) were synthesized using β -thiopropionate-polyethylene glycol (PEG) as the gatekeeper. The study's findings indicated that the medium pH, concentration, and packaging of βthiopropionate-PEG were the main factors controlling drug release. The introduction of folic acid (FA) to the shell-core Fe₃O₄@mSiO₂-DOX@-Se-Se-FA demonstrated effective doxorubicin (DOX) encapsulation [11]. The addition of FA enhanced both cell uptake and release. Madrid et al. [12] used both hydrothermal and sol-gel methods to make Fe3O4@mSiO2 nanocomposites with different shell thicknesses. The drug ibuprofen was used to assess the efficacy of intake and liberation. This study revealed a relationship between surface area, load of drugs, and outer shell thickness. Jiang et al. [13] mixed Fe₃O₄@mSiO₂@LDH NPs and chose layered double hydroxide (LDH) to control how fast the particles could be released. These MNPs were found to exhibit reasonable loading proportions, and for better 72 hours, the release rates of methotrexate MTX-loaded MNPs were adjusted based on the pH level. To increase stability, Cicily [14] prepared mesoporous core-shell Fe₃O₄@mSiO₂ nanoparticles by applying surfactants as a template in the sol-gel process and using them as additives in a carbonyl iron-based magnetorheological system. Iranpour et al. [15] designed a novel drug delivery system utilizing magnetized mesoporous silica core-shell nanoparticles (SPION@MSNs), where gold gatekeepers prevented the escape of doxorubicin (DOX) at physiological pH. They created mesoporous silica nanoparticles with or without a magnetic core using a hydrothermal process, which they then used as norfloxacin (NFX) carriers. Batch experiments have been used to study the kinetics of NFX release. In all cases, the localization of NFX on the exterior surface of the nanoparticles led to the rapid extraction of more than 55% of the antibiotic within the first five minutes [16]. The goal of this study is to use magnetic Fe₃O₄ that has already been made as the core and mesoporous silica mSiO2 as the shell (Fe₃O₄@mSiO₂) to look into how DPH drugs are absorbed from water solutions and how well they can be loaded onto the Fe₃O₄@mSiO₂ carrier. The drugs will then be released in vitro.

2. Experimental

2.1. Chemicals

The Iraqi state company of vegetable oils provided the template, carbomidopropyl betaine (CABP), as well as the silica precursor form, sodium silicate (14% NaOH, 27% SiO₂). The antibiotic Diphenhydramine (DPH) was provided by DSM with a purity 98%), M.wt. 255.355

g/mol, λ_{max} = 221 nm, in a water-based solution, as seen in Figure 1, which also illustrates its structure.

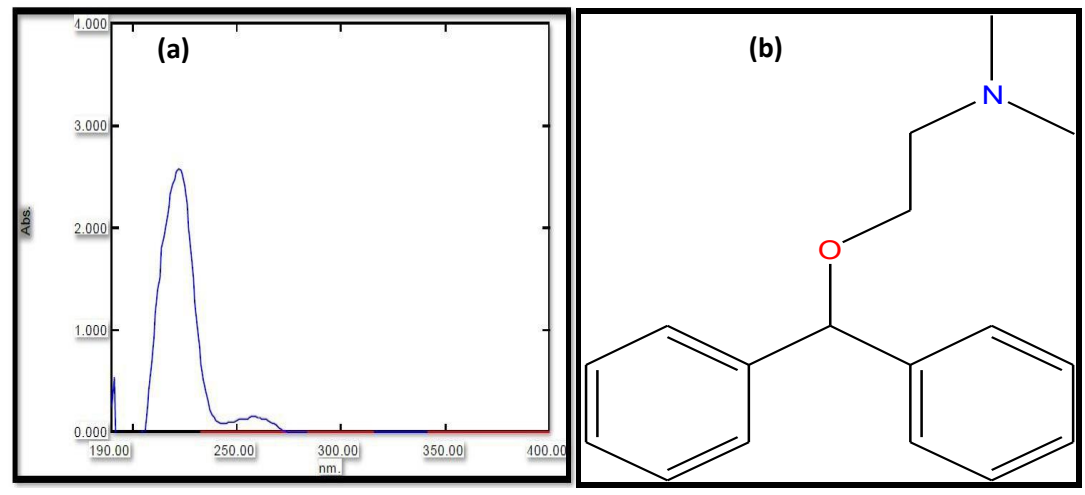


Figure 1: UV-Vis absorption spectra (a) for the chemical structure (b) for DPH

2.2. Preparation of adsorbent

The method previously reported [17] is similar to the procedure for preparing magnetite Fe₃O₄ and the Fe₃O₄@mSiO₂ adsorbent. Magnetic Fe₃O₄ was prepared as follows: 0.9 g of urea (BDH:England: 99%), was dissolved in 60 mL of mixed solvent (2:58 mL of water and ethylene glycol) (HIMEDIA; 99%) and FeCl₃.6H₂O (0.54 g) (HIMEDIA: 98%) was added with stirring at 40 °C until totally dissolved. The mixture was poured into a 100-mL Teflon-line autoclave, heated it to 200 °C, and preserved it for 24 hours. After cooling, the mixture was centrifuged, separated, washed, and dried at 80 °C for 6 hours in an oven. Preparation of Fe₃O₄@mSiO₂ was done by weighting Fe₃O₄ (10 mg), which was dispersed in ethanol (50 mL) under ultrasonic agitation. The Fe₃O₄ was separated and mixed with CABP surfactant (12 g), H₂SO₄ (17 mL, 1.0 M), and water (150 mL). Sodium silicate (3.5 g) dissolved in distilled water (150 mL) was added to the mixture drop-by-drop from the burette for 3 hours. The solution was left at room temperature for one day, and then the precipitate formed was recovered by filtration and washed with distilled water. The precipitate was dried at 80 °C for 2 hours and calcined at 600°C for 5 hours.

2.3. Adsorption study

Using 100 mL of an aqueous solution with different concentrations of DPH (2, 8, 14, 20, 26, 32, 38, 44, and 50 mg/L) and the adsorbent Fe₃O₄@mSiO₂ (0.06 g), the adsorption isotherm was evaluated. To achieve equilibrium, the DPH-Fe₃O₄@mSiO₂ mixture system underwent vigorous shaking for 110 minutes. Then, the DPH solution (2 mL) was taken out and centrifuged for 15 minutes to find out how concentrated the DPH solution was before and after adsorption. This was done by measuring the UV-Vis absorption value at λ max 221 nm. The following equation was used to *calculate* how much DPH was adsorbed:

$$q_e = \frac{(C_0 - C_e) V}{w} \qquad \dots \dots (1)$$

Where, C_0 is the initial DPH concentration (mg L^{-1}), Ce is the concentration at equilibrium, v is the volume of DPH solution (L), and W (g) is the adsorbent's weight. Furthermore, q_e represents the equilibrium adsorption of DPH on the unit mass of the adsorbent. The removal percentage, or R%, was calculated using the following formula:

$$R\% = \frac{c_0 - c_e}{c_0} \times 100 \qquad \dots \dots (2)$$

2.4. Drug loading

By applying a modified method described in the literature [13], the DPH loading capacity of the prepared Fe₃O₄@mSiO₂ was tested; Fe₃O₄@m-SiO₂ (30 mg) was transferred into a container containing DPH medication solution (5 mL of 100 mg/mL), and the mixture was stirred for 24 hours. After that, the precipitate was separated by centrifuging it for 15 minutes and drying in an oven for 24 hours at 60 °C.

2.5. *In vitro drug-release*

The DPH-Fe₃O₄@mSiO₂ sample (30 mg) has been placed in water (100 mL) or PBS (pH = 7.4) with a stirrer at 37.5 °C. One mL of aliquots was taken from the solution at time intervals, and the quantity of DPH released has been estimated using the aliquots' UV-Vis absorption spectra.

3. Results and discussion

3.1. Adsorption study

3.1.1. Effect of equilibrium time and dosage of adsorbent

The influence of equilibrium time and adsorbent dose on DPH adsorption on Fe₃O₄@mSiO₂ was investigated for DPH solutions containing 20 mg L⁻¹ and at 298 K (Figure 2).

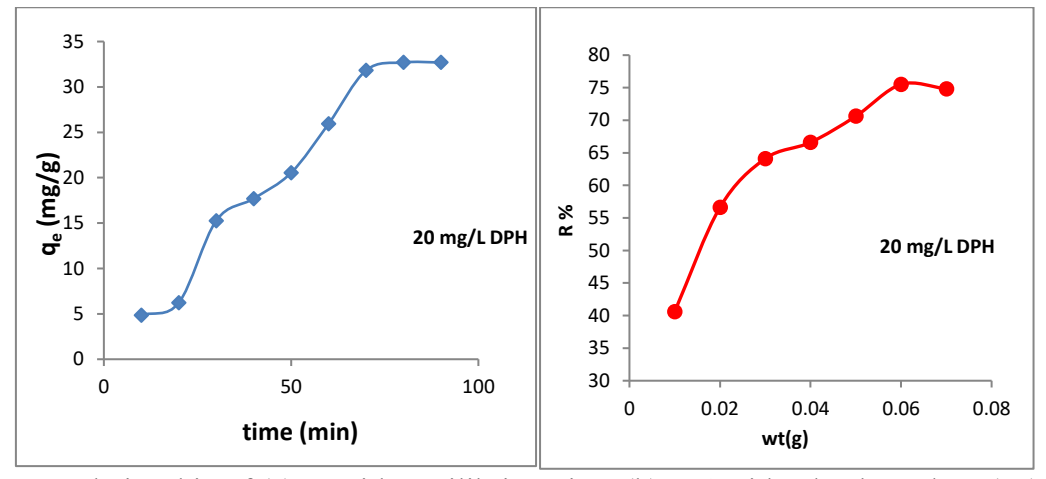


Figure 2: Relationship of (a) q_e with equilibrium time (b) R% with adsorbent dose (wt) at 100 minutes for DPH adsorption at 298 K

Adsorption increases gradually as contact time is increased to one hundred minutes; therefore, the time of 100 minutes is fixed as the optimum contact time. To study the impact of adsorbent weight, different amounts of adsorbent (0.01, 0.02, 0.03, 0.04, 0.05, 0.06, and 0.07 g per 100 mL) were added to the test solution over a 100-minute period of time. The drug's percentage removal (R%) increases as the adsorbent dosage increases, but beyond a value of 0.06 g, the degree of removal approaches a maximum. This is most likely because of the increased availability of exchangeable sites or the increased surface area where adsorption occurs; this could also be attributed to adsorbent aggregation and the increased availability of surface active sites caused by the raised dose [18-19]. As a result, 0.06 g of adsorbent was used in all subsequent experiments.

3.1.2. Adsorption isotherm

The isotherms of four adsorption theories, Langmuir (Equation 3), Freundlich (Equation 4), Temkin (Equation 5), and Dubinin-Radushkevich (Equation 6), have been displayed (Figuer 7) using an ordinary straight line formula, and the associated adsorption parameters have been determined from the corresponding plots:

$$\frac{C_e}{q_e} = \frac{1}{K_L \cdot q_m} + \frac{C_e}{q_m} \qquad(3)$$

$$\ln q_e = \ln K_f + \frac{1}{n} \ln C_e \qquad \dots \dots (4)$$

$$q_e = B \ln K_T + B \ln C_e \qquad \dots \dots (5)$$

$$lnq_e = (lnq_m - \beta \epsilon^2) \qquad \dots \dots (6)$$

Where B = RT / b and b is an equilibrium constant, β is connected to mean adsorption energy E (J/mol) via the formula $E = (-2 \beta)^{-0.5}$, and ϵ is the Polanyi potential defined as $\epsilon = RT \ln (1 + 1/C_e)$. The constants K_L , q_m , K_F , 1/n, B, K_t , and β are associated with the Timken constant, the maximum amount of adsorption that may occur, the quantity of adsorption that can occur, the intensity of adsorption, and the Langmuir adsorption equilibrium constant. Table 1 contains the values obtained for the parameters.

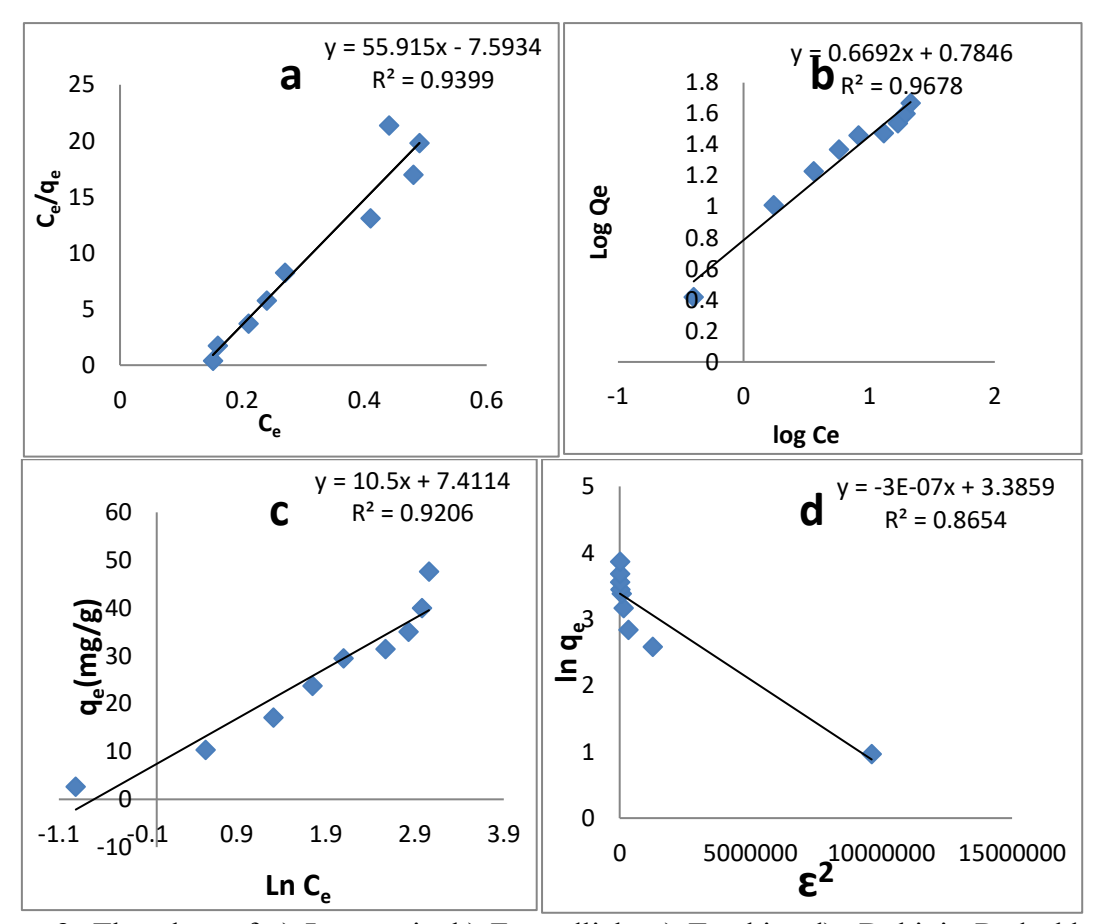


Figure 3: The plots of a) Langmuir, b) Freundlich, c) Temkin, d) Dubinin-Radushkevich models at 293 K

Tuble 1: The four models parameters for B111 adsorption on 1 6,0460ms102								
I an amazin	$q_m \ (mg/g)$	$K_L (mg/l)^{-1}$	R_{L}	\mathbb{R}^2				
Langmuir	59.52	0.114	0.149	0.9399				
E 41: -1.	1/n	K_f (L. g^{-1})	\mathbb{R}^2					
Freundlich	0.669	2.190	0.9678					
	B (L/mg)	$K_T(J/mol)$	\mathbb{R}^2					
Temkin,	10.505 2.022		0	.9206				
Dudinia Dadaaldaasid	B (mol ² J ⁻²)	q _m (mg/g)	E (kJ/mol)	R ²				
Dubinin-Radushkevich	-3×10 ⁻⁶	38.97	0.40	0.8654				

Table 1: The four models' parameters for DPH adsorption on Fe₃O₄@mSiO₂

Results of Table 1 indicate that R² values were high for the three isotherms (Langmuir, Freundlich, and Temkin), but the isotherm is best fitted by the Freundlich model, which may be appropriate for describing the loading of DPH on Fe₃O₄@mSiO₂. The drug may absorb more favorably when 1/n is less than 1. When n falls between 1 and 10, as well as 1/n between 0 and 1, it means that the conditions of heterogeneity and positive cooperativeness are met [20]. The Dubinin-Radushkevich isotherm for the DPH drug adsorption process on Fe₃O₄@mSiO₂ yields an E value of 0.04 kJ/mol. This value, being lower than 8 kJ/mol, indicates that the adsorption process is of the physical adsorption type [21].

3.1.3. Adsorption kinetic

Three of the most popular kinetic models are utilized to analyze the adsorption kinetic behavior of the DPH drug onto Fe₃O₄@mSiO₂ at 298 K: pseudo first order of Lagergren (equation 7), the pseudo-second order equation (Equation 8) and the intraparticle diffusion equation (Equation 9). Table 2 and Figure 4 illustrate the outcomes of these equations.

$$ln(q_e - q_t) = lnq_e - k_1 t \qquad \dots (7)$$

$$\frac{t}{q_t} = \frac{1}{k_2 q_e^2} + \left(\frac{1}{q_e}\right) t \qquad(8)$$

$$q_t = k_D t^{0.5} + C$$
(9)

The pseudo-first order model (min⁻¹) has a rate constant k_1 , while the pseudo-second order model (mg.min⁻¹) has a rate constant k_2 . Here, q_e represents the adsorption capacity (mg.g⁻¹) at equilibrium, and q_t represents time t. The initial adsorption rate in this case is $h = k_2 q_e^2$. The intercept is denoted by C, and the intrapartical diffusion rate constant is given by k_D (mg g⁻¹ min^{-1/2}). Together with the h value, which is given in Table 2, the constants q_e , k_1 , k_2 , and k_D are computed using the values of the slopes and intercepts of the linear plots of the three equations (Figure 4).

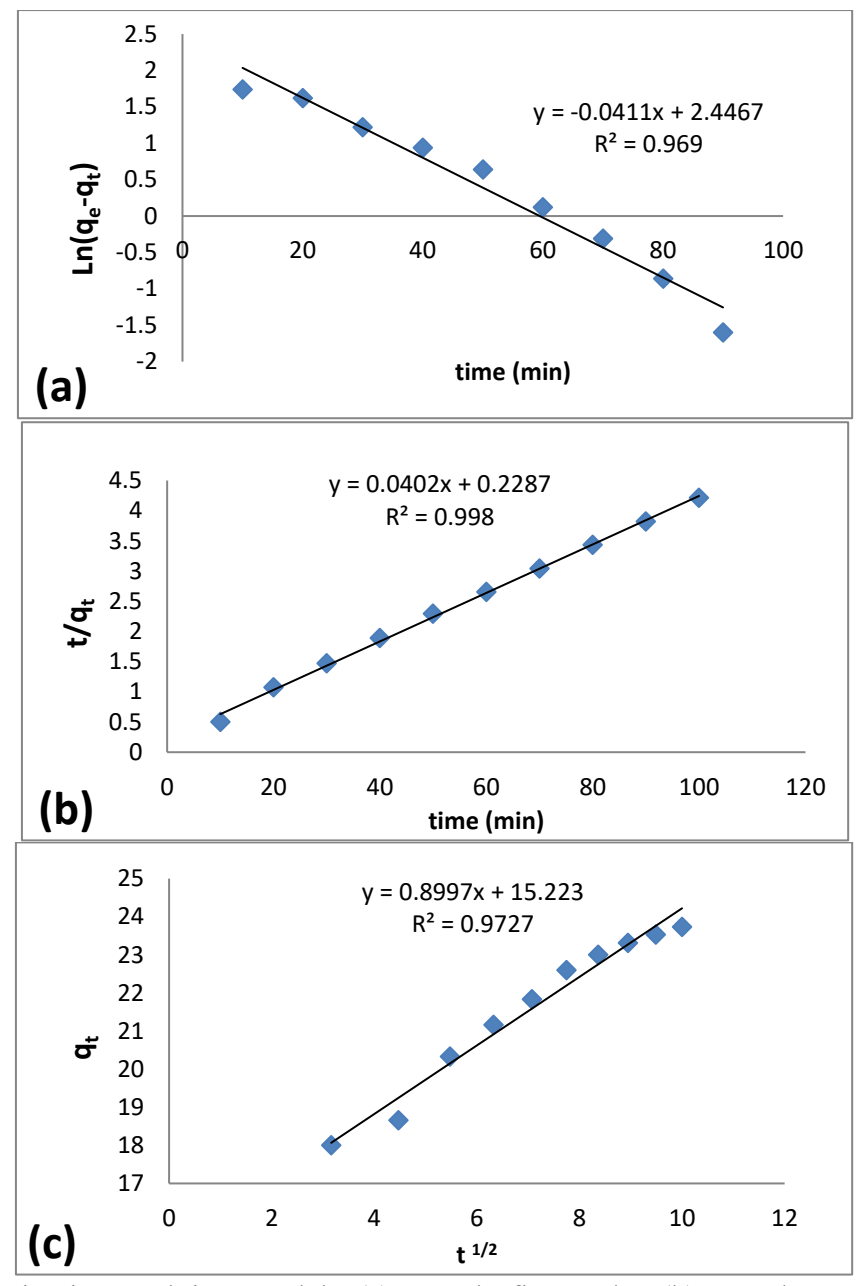


Figure 4: Kinetics applying models (a) pseudo-first order (b) pseudo-second order (c) intraparticle diffusion

According to the correlation coefficient (R²) values in Table, the adsorption follows the pseudo-second-order model. The plot of the intra-particle diffusion model also reveals a higher drug absorption rate in the first linear portion and a lower rate in the second linear portion, likely due to diffusion through tiny pores and the subsequent attainment of equilibrium. The figure for the intra-particle diffusion model also shows that the straight line at extrapolation did not reach the origin. This means that other steps besides the intraparticle diffusion step have a big effect on the rate [22,23].

q _e	First order			Second order				Intrapartical diffusion	
(mg/g) (exp.)	q _e (calc) (mg/g)	K ₁ (min ⁻¹)	\mathbb{R}^2	q _e (calc) (mg/g)	K ₂ mg g ⁻¹ min ⁻¹	h ((mg g- ¹ min- ¹)	\mathbb{R}^2	$\begin{array}{c} K_D \\ (mg~g^1min^{\text{-}1/2}) \end{array}$	\mathbb{R}^2
23.73	11.54	0.041	0.969	25	7.01×10 ⁻³	4.38	0.998	1.049	0.972

Table 2: Kinetic parameters for adsorption of DPH drug on Fe₃O₄ @mSiO₂ at 298K

3.2. Study the loading and release of the drug DPH

The equation that follows has been used to calculate the quantity of drugs loaded [24].

Loading
$$(mg_{drug} / mg_{sample}) = \frac{m(DPH.orig) - m(DPH.solution)}{m (sample)} \dots (10)$$

The original amount of DPH drug in 5 mL of solution represents (m_{DPH orig}) while its amount in the solution after impregnation for 24 hours is m_{DPHsolution} and m_{sample} is the weight of the Fe₃O₄@mSiO₂ sample. The DPH loading in the samples was calculated to be 13.33 mg drug/mg sample. Our adsorbent's loading capacity is equivalent to that of other adsorbents-drug reported [13,25]. Figure 5 exhibits the release characteristics of the loaded Fe₃O₄@mSiO₂ sample in water and a PBS solution for a period of 90 minutes. Using absorption spectra, the amount of DPH released in the PBS and water solution was calculated. It is evident that after 90 minutes, the Fe₃O₄@mSiO₂ sample released roughly 57.23 and 97.27% of the DPH drug in water and PBS solution, respectively. Additionally, the prepared sample Fe₃O₄@mSiO₂'s porous external surface initially releases DPH at a rapid rate for the first 60 minutes in water media and 40 minutes in PBS medium, before a progressive release rate takes effect. The strong capillary force could be the cause of the drug's weak release within the mesoporous material.

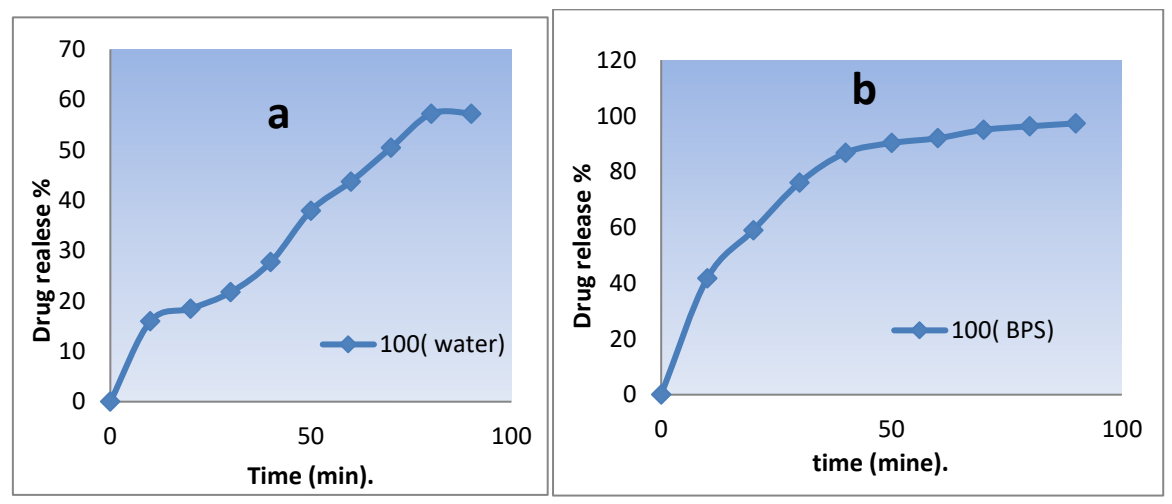


Figure 5: The release profile of DPH-loaded Fe₃O₄@mSiO₂ in (a) water, (b) PBS at 37 °C

3.3. Kinetic of drug releasing

Three models were fitted to the data of in vitro drug release in order to explore the kinetics of drug release from the carrier: Korsmeyer-Peppas, first-order kinetic release, and Kopcha.

The Korsmeyer-Peppas [27] model is the first one [equation (11)] [24]. M_t is the amount of drugs released at time t in minutes, M_{∞} is the amount of drugs loaded into mSiO₂ particles, $k_{\rm K-P}$ is the kinetic constant for the host-guest pair, and n is the shape of the host and how the drugs are released. The second model is first order kinetic release model [28] (eq.12) where k is the first order rate constant. The third model, known as the Kopcha model [29], represents the contributions of erosion (B) and diffusion (A). The primary property of a drug delivery system that characterizes it is kinetics is drug release, which establishes the drug release mechanism. In this study, Korsmeyer - Peppas, psedo First-order and Kopcha Kinetics models of DPH drug release from of the carrier; Fe₃O₄@mSiO₂were studied by fitting the *in vitro* drug release data. The obtained kinetic curves in water and PBS were presented in Figures 6 and 7. The Kinetic parameters determined from the slope and intercept of the three models in water and PBS media are listed in Table 3.

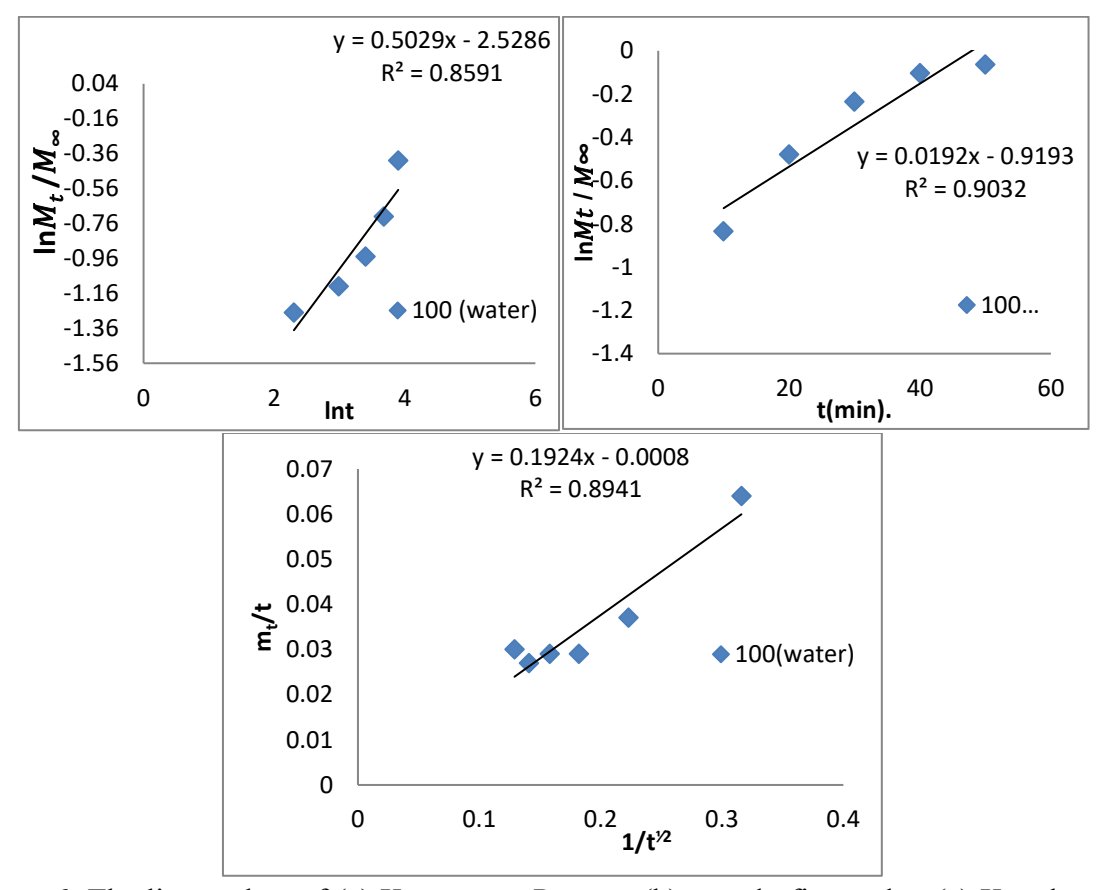


Figure 6: The linear plots of (a) Korsmeyer-Peppas, (b) pseudo-first order, (c) Kopcha order model kinetics releasing model for the DPH drug in water

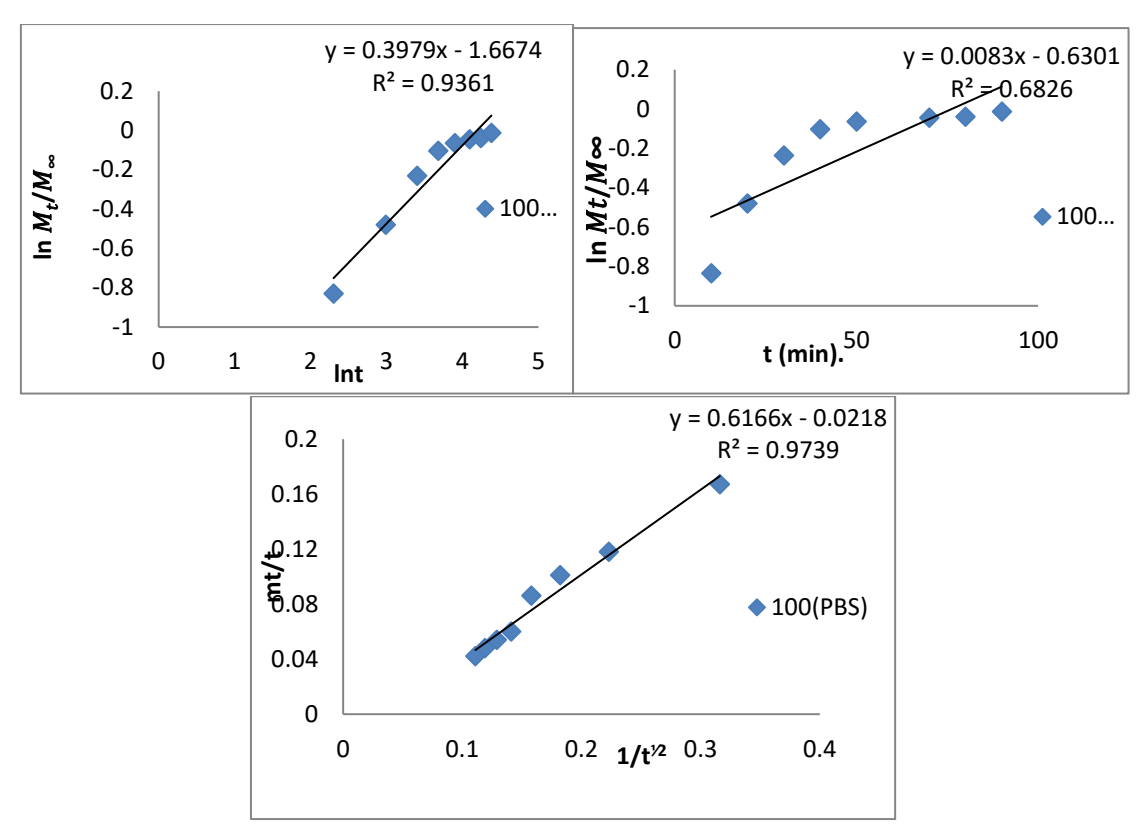


Figure 7: The linear plots of (a) Korsmeyer – Peppas, (b) pseudo-first order, (c) Kopcha order model kinetics releasing model for the DPH drug in PBS

Table 3: The estimated parameters for the kinetic release of DPH drug-loaded Fe₃O₄@mSiO₂ in water and PBS media

Model	Korsmeyer-Peppas			Pseudo-first order		Kopcha Model		
parameters	n	K_{I}	\mathbb{R}^2	K	\mathbb{R}^2	A	В	\mathbb{R}^2
(PBS)	0.3979	0.188	0.9361	0.0083	0.6826	0.6166	-0.0218	0.9739
(Water)	0.618	0.055	0.9010	0.020	0.987	0.167	0.005	0.849

DPH-Fe₃O₄@mSiO₂ carrier release kinetics show that the kopcha and Korsmeyer-Peppas models in PBS media and the pseudo-first-order model in water media have a high value of R^2 . The results of Table 3 indicate that the Kopcha model conforms more closely to the data release than other models. In PBS media, the values of n (the Korsmeyer-Peppas constant) are less than 0.43 for the drug-carrier systems, showing a Fickian diffusion release. However, in water media, the values are 0.43 < n < 0.85, showing that the release is an anomalous diffusion release. The ratio of A to B determines the primary release mechanism in kopcha. When A/B is greater than 1, diffusion controls the primary release mechanism, and when A/B is less than 1, erosion controls it. When the release mechanism is set to 1, diffusion and erosion coexist [30]. In this study, the drug release in both media exhibits an A/B value greater than 1, indicating that diffusion controls the release mechanism.

4. Conclusion

According to the study's previous outcomes, the Freundlich model best described the data, and Fe₃O₄/mSiO₂ nanoparticles were an efficient adsorbent for the adsorptive removal of DPH drugs from aqueous solutions. The loading study found that 97.27% of the drug that was loaded in PBS solution was released. This means that it is a good DPH drug carrier, with a capacity of 13.33 mg drug/mg sample. Drug release kinetics demonstrates that diffusion controls the

release mechanism, and that the Kopcha model matches the data release more closely than other models.

References

- [1] A. Al-jubori, A. T. Tawfeeq, and G. M. Sulaiman, "Novel tamoxifen citrate-loaded polymeric nanoformulations for improving treatment and uses in medical applications: An in vitro and in vivo study", *Iraqi Journal of Science*, vol. 63, no. 6, pp. 2419-2433, 2022.
- [2] K. Albinali, M. Zagho, Y. Deng, and A. Elzatahry, "A perspective on magnetic core–shell carriers for responsive and targeted drug delivery systems", *International Journal of Nanomedicine*, vol. 14, pp. 1707-1723, 2019.
- [3] Nanocarriers for Drug Delivery: Concepts and Applications. S.l.: SPRINGER NATURE, 2022.
- [4] W. N. Kadhum and Israa A. Z. Al-Ogaidi, "Evaluation of chitosan-alginate nanoparticle as a stable antibacterial formula in biological fluids", *Iraqi Journal of Science*, vol. 63, no. 6, pp. 2398-2418, 2022.
- [5] S. Zhao, S. Zhang, J. Ma, L. Fan, C. Yin, G. Lin, and Q. Li, "Double loaded self-decomposable SiO₂ nanoparticles for sustained drug release", *Nanoscale*, vol. 7, no. 39, pp. 16389-16398, 2015.
- [6] C. Argyo, V. Weiss, C. Braeuchle, and T. Bein, "Multifunctional mesoporous silica nanoparticles as a universal platform for drug delivery", *Chemical Material*, vol. 26, no. 11, pp. 435-451, 2014.
- [7] F. Liu, J. Wang, P. Huang, Q. Zhang, J. Deng, Q. Cao, J. Jia, J. Cheng, Y. Fang, D. Y. Deng, and W. Zhou, "Outside-in stepwise functionalization of mesoporous silica nanocarriers for matrix type sustained release of fluoroquinolone drugs", *Journal of Materials Chemistry B*, vol. 3, no. 10, pp. 2206-2214, 2015.
- [8] S. Wu, X. Huang, and X. Du, "PH- and redox-triggered synergistic controlled release of a zno-gated hollow mesoporous silica drug delivery system", *Journal of Materials Chemistry B*, vol. 3, no. 7, pp. 1426-1432, 2015.
- [9] G. K. Nasrallah, Y. Zhang, M. M. Zagho, H. M. Ismail, A. A. Al-Khalaf, R. M. Prieto, K. E. Albinali, and A. Ahmed, "A systematic investigation of the bio-toxicity of core-shell magnetic mesoporous silica microspheres using zebrafish model", *Microporous and Mesoporous Materials*, vol. 265, pp. 195-201, 2018.
- [10] C. Yang, W. Guo, L. Cui, N. An, T. Zhang, H. Lin, and F. Qu, "PH-responsive magnetic coreshell nanocomposites for drug delivery", *Langmuir*, vol. 30, no. 32, pp. 9819-9827, 2014.
- [11] N. An, H. Lin, C. Yang, T. Zhang, R. Tong, Y. Chen, F. Qu, "Gated magnetic mesoporous silica nanoparticles for intracellular enzyme-triggered drug delivery", *Materials Science and Engineering: C*, vol. 69, pp. 292-300, 2016.
- [12] S. I. Uribe Madrid, U. Pal, Y.S. Kang, J. Kim, H. Kwon, and J. Kim, "Fabrication of Fe₃O₄@mSiO₂ core-shell composite nanoparticles for drug delivery applications", *Nanoscale Research Letters*, vol. 10, Article no. 215, 2015.
- [13] W. Jiang, J. Wu, R. Tian, and W. Jiang, "Synthesis and characterization of magnetic mesoporous core—shell nanocomposites for targeted drug delivery applications", *Journal of Porous Materials*, vol. 24, no. 1, pp. 257-265, 2016.
- [14] S. Gopi, P. Balakrishnan, and N. M. Mubarak, "Nanotechnology for Biomedical Applications. Singapore: Springer Nature, 2022.
- [15] S. Iranpour, A. R. Bahrami, S. Nekooei, A. Sh. Saljooghi, and M. M. Matin, "Improving anticancer drug delivery performance of magnetic mesoporous silica nanocarriers for more efficient colorectal cancer therapy", *Journal of Nanobiotechnology*, vol. 19, Article no. 314, 2021.
- [16] Z. Li, Y. Zhang, and N. Feng, "Mesoporous silica nanoparticles: Synthesis, classification, drug loading, pharmacokinetics, biocompatibility, and application in drug delivery", *Expert Opinion on Drug Delivery*, vol. 16, no. 3, pp. 219-237, 2019.
- [17] E. Abdul Hussein and S. H. Kareem, "Magnetic mesoporous silica material (Fe₃O₄@mSiO₂) as adsorbent and delivery system for ciprofloxacin drug", *IOP Conf. Ser.: Materials Science and Engineering*, 871012020, 2020.
- [18] Y. Z. Chunyan, L. Lidong, W. Kangjun, Z.Yuan, B. Jiaqi, and W. Jing, "Solvothermal synthesis of mesoporous Fe₃O₄ nanoparticles in mixed solvent of ethylene glycol and water: structure and

- magnetic properties", Journal of Superconductivity and Novel Magnetism, vol. 32, pp. 757-762, 2019.
- [19] M. Barbooti, K. Al-Bassam, and B. Qasim, "479 evaluation of Iraqi montmorillonite as adsorbent for the removal of oxytetracycline from water", *Iraqi Journal of Science*, vol. 53, no. 3, pp. 479-486, 2024.
- [20] J. H. Hassen, M. S. Ferhan, and A. H. Ayfan, "Fexofenadine adsorption by activated charcoal impregnated with hydrogen peroxide", *Iraqi Journal of Science*, vol. 61, no. 6, pp. 1245-1252, 2020.
- [21] T. J. Dening, D. Zemlyanov, and L. S. Taylor, "Application of an adsorption isotherm to explain incomplete drug release from ordered mesoporous silica materials under supersaturating conditions", *Journal of Controlled Release*, vol. 307, pp. 186-199, 2019.
- [22] N. Nasuha, B. H. Hameed, and A. T. Din, "Rejected tea as a potential low-cost adsorbent for the removal of methylene blue", *Journal of Hazardous Materials*, vol. 175, no. 1-3, pp. 126-132, 2010.
- [23] S. Chowdhury, S. Chakraborty, and P. Saha, "Biosorption of basic green 4 from aqueous solution by Ananas comosus (pineapple) leaf powder", *Colloids and Surfaces B: Biointerfaces*, vol. 84, no. 2, pp. 520-527, 2011.
- [24] N. R. Biswal and S. Paria, "Effect of electrolyte solutions on the adsorption of surfactants at PTFE-Water Interface", *Industrial and Engineering Chemistry Research*, vol. 49, no. 15, pp. 7060-7067, 2010.
- [25] H. Alp, M. Ince, O. Kaplan Ince, and A. Onal, "Biosorptive removal of eriochrome black-T using Agaricus campestris: parameters optimization with response surface methodology", *Desalination and Water Treatment*, vol. 175, pp. 244-254, 2020.
- [26] X. Mei, D. Chen, D. Li, Q. Xu, J.Ge, H. Li, B. Yang, Y. Xu, and J. Lu, "Facile preparation of coating fluorescent hollow mesoporous silica nanoparticles with ph-sensitive amphiphilic diblock copolymer for controlled drug release and Cell Imaging", *Soft Matter*, vol. 8, no. 19, p. 5309, 2012.
- [27] R. W. Korsmeyer, S. R. Lustig, and N. A. Peppas, "Solute and penetrant diffusion in swellable polymers. I. Mathematical Modeling", *Journal of Polymer Science Part B: Polymer Physics*, vol. 24, no. 2, pp. 395-408, 1986.
- [28] P. Shende and S. Govardhane, "Strategies-based intrathecal targeted drug delivery system for effective therapy, modeling, and controlled release action", *Modeling and Control of Drug Delivery Systems*, pp. 213-225, 2021.
- [29] M. Kopcha, K. J. Tojo, and N. G. Lordi, "Evaluation of methodology for assessing release characteristics of thermosoftening vehicles", *Journal of Pharmacy and Pharmacology*, vol. 42, no. 11, pp. 745-751, 1990.
- [30] N. Shahabadi, M. Falsafi, and K. Mansouri, "Improving antiproliferative effect of the anticancer drug cytarabine on human promyelocytic leukemia cells by coating on Fe₃O₄@SiO₂nanoparticles", *Colloids and Surfaces B: Biointerfaces*, vol. 141, pp. 213-222, 2016.